Journal of Microelectronics and Electronic Packaging (2013) **10**, 80-88
Copyright © International Microelectronics And Packaging Society
ISSN: 1551-4897

Combined Temperature and Vibration Testing for Wire Bond Interconnections in Harsh Environment Electronics

M. Mirgkizoudi,[1,*] C. Liu,[1] P. P. Conway,[1] and S. Riches[2]

***Abstract*—The performance of electronics in harsh environments is often affected by a combination of environmental factors. Qualification tests on such electronics are normally carried out by separate environmental tests such as temperature storage, temperature cycling and vibration tests. This approach may miss the effects of combined parameters, where for example, there may be degradation in a vibration environment that may be accelerated by temperature related effects on material properties.**

This paper presents results from a study of the combined effects of temperature and vibration on wire bonded interconnections that are used in the production of high temperature electronic components. The study is focused on the testing of electronic components under the combination of temperature exposure up to 250°C and vibration loading with a frequency range between 500 Hz and 2,000 Hz and acceleration up to 20 G_{rms}. The study covers aspects of wire bond connections and their failure mechanisms, where the effect of wire loop height and length under separate and combined vibration and temperature tests has been investigated. The study has also assessed the effect on packaged Silicon on Insulator (SOI) devices assembled into ceramic packages under representative combined temperature and vibration profiles. The work has shown that the combined effect of temperature and vibration has increased the susceptibility of wire bond interconnections to vibration-induced failures.

***Keywords*—High temperature, vibration, wire bonding**

Introduction

Wire bonding of microelectronic packages has been used industrially for more than 40 years. Au, Al, and Cu wires are widely used in various microelectronic systems [1]. However, the exposure of such systems in extreme environments can significantly affect their reliability and lifetime; such harmful environments may include high and low temperatures, humidity, pressure, radiation, external stresses and vibration loadings [2].

The reliability of electronics interconnects is one of the greatest concerns in high temperature applications. The main focus has been on the failures occurring during thermal cycling and high temperature exposure. The reliability of wire bonded devices at high temperature conditions has been thoroughly investigated. Shepherd et al. [3] examined the changes in bond mechanical behavior and the underlying microstructural stability of Au-Au wire bonds arising from thermal ageing. Using wire pull and ball shear tests, they observed a decrease in yield strength after only a few hours of testing. Bahi et al. [4] developed a methodology for "in situ" monitoring of wire bond degradation during high-temperature ageing tests for standard plastic packages. In this method the onset wire-bond degradation is identified through the progressive increase in their resistance. Reliability concerns on wires subjected to thermal ageing also arose in the work of Agyakwa et al. [5]. After investigation of the suitability of ultrasonic wire bonding in high temperature applications and collection of shear testing, indentation hardness and fine-scale microstructural data, they reported that the degradation rate can be influenced by the maximum temperature and duration at which the wire bonds are exposed. They suggested that high purity Al wire bonds could be used as a reliable solution for high temperature operations above 125°C. Mayer et al. [6] developed a microsensor application for real-time signal recording of the stress caused by ball bond during long-term high-temperature storage tests. The sensor is capable of identifying stresses from thermal expansion mismatch, recovery and recrystallization mechanisms caused by temperature changes, and ageing mechanisms of the ball bonds. The reliability of ball bond and the effect of post bond high temperature storage have also been investigated by Murali et al. [7]. As a case study of their work they investigated the interface morphology and metallurgical behavior of Au and Cu ball bonds for different wire diameters and thermal ageing periods. They found that Au wires on Al metallization are more susceptible to void formation; the phenomenon was mostly observed in finer wires. They also found that Cu wires bonded on Al metallization are more reliable at elevated temperatures up to 300°C due to good diffusional bonding and the absence of intermetallic phase formation. Long-term temperature reliability of wire bonds has also been investigated by Oldervoll and Strisland [8]. Their work focused on improving Al wire bonding to ceramic thick films. They reported that Al to Ag thick film plated with Cu and Ni is a better solution from Au to Pd thick film due to better mechanical strength and unaltered electrical resistance after thermal ageing. Degradation is another issue of concern. Mustain et al. [9] investigated the Al and Au wire bonding processes for high temperature electronics. They suggested that the bonding pad and the wire should be of the same material due to the degradation of the bond strength caused by interdiffusion and interface corrosion between dissimilar metals at high temperatures.

Manuscript received on April 22, 2013; revised on May 20, 2013; accepted on May 23, 2013

[1]Wolfson School of Mechanical & Manufacturing Engineering, Loughborough University, Loughborough, LE11 3TU, UK
[2]GE Aviation Systems-Newmarket, 351 Exning Road, Newmarket, Suffolk, CB8 0AU, UK
*Corresponding author; email: M.Mirgkizoudi@lboro.ac.uk

Downloaded from http://meridian.allenpress.com/jmep/article-pdf/10/2/80/2240810/imaps_376.pdf by guest on 31 October 2022

By contrast, the combined effects of thermal and mechanical loadings on wire bonds have received comparatively little attention. As reported in our previous work, vibration combined with thermal loading can cause severe damage on the wires and wire bonds of electronic packages [10]. Bending and distortion of wires due to the extreme conditions applied can cause failure by short circuits. Some failures at the interfaces between the wires and the chip and substrate were also observed. The interfacial failure at the wire bonds, and subsequent lift-off was found mostly on the interconnections with the substrate. In another one of our previous papers [11] the orientation of the wire bonded devices in respect to the direction of the vibration has also been investigated. It has been demonstrated that the distortion and subsequent failure is more severe when the wires are vertically oriented to the direction of the vibration. Failure modes such as wire lift-offs and short circuits occur more often in this case.

This paper reports a further investigation into the effects of the combined extreme conditions on wire bonded devices. A series of tests have been performed at various temperature, frequency and acceleration levels to determine the effects of each factor on the system. Preliminary data on the effect on the gain of SOI (Silicon on Insulator) op-amps vibration tested at 25°C and 250°C is also presented.

Methodology

Wire Bonding

This work focused on Au ball/wedge bonding on substrates with Au thick film metallized pads and ceramic bases. The substrates, supplied by GE Aviation Systems, had a 1mm thick Al_2O_3 ceramic base with four integrated 10 μm thick Au thick film pads, as shown in Fig. 1. In order to investigate how the wire loop geometry is affected by the conditions applied, two different bonding profiles have been applied. The four pads were wire bonded by pairs of two (see Fig. 1). One pair was used to form wire bonds with small wire loop height and the other with large wire loop height. Each pair consisted of a row of 15 bonds.

The diameter of the Au wire used for the wire bonding process was $D_w = 25$ μm and the ball bond diameter was $D_b = 75$ μm. The small wire loop height was set to be $h_1 = 200$ μm and the large $h_2 = 270$ μm. The space between the bonds in the rows was 300 μm. Fig. 2 shows a schematic representation of the wire bonding structure.

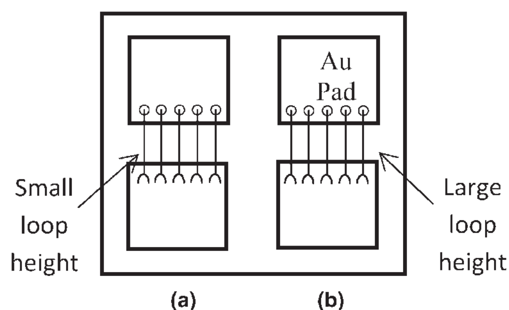

Fig. 1. Schematic representation of the two wire bonding profiles for (a) the small loop height ($h_1 = 200$ μm), and (b) the large loop height ($h_2 = 270$ μm).

The devices were thermosonically bonded using the Kulicke & Soffa 4500 wire bonder. Table I contains the bonding parameters as set for the two wire loop heights. As seen in Table I, the wire bonding levels of parameters differ for the two bonding profiles. During the wire bonding process it has been observed that the parameters for the small loop wires were not suitable for those that form a large loop; the loop shape was deformed and the formation of a parabolic loop shape could not be achieved. Thus, the levels of the parameters were adjusted in order to achieve the desired results.

The cleaning protocol summarized in Fig. 3 was used to clean the substrates prior to wire bonding. The protocol consisted of a series of steps where Decon 90 and de-ionized (DI) water were used. Inspection of the devices under microscope followed in order to assure a clean interface between the Au thick film pads and the bonds.

Experimental Details

A testing protocol was developed to examine the combined effects of temperature and vibration based on a factorial design of experiments. In terms of the thermal conditions, the only factor was the temperature that was kept constant during the tests and at two different levels; either at 120°C or at 250°C. The vibration parameters—frequency and acceleration—were also applied at two levels each. For the frequency, the levels were 500 Hz and 2,000 Hz, and for the acceleration, 10 G_{rms} and 20 G_{rms}, which produced a 2^3 experiment (3 factors at 2 levels each).

This led to an experimental design that consisted of eight runs—eight different combinations of testing conditions. Table II presents those combinations of the control factors and their levels. Here A, B, and C are the temperature, frequency, and acceleration respectively. The symbols (−) and (+) represent the lower and the higher levels of the control factors. As it was said above, these are:

A: Temperature level: 250°C (+) and 120°C (−)
B: Frequency level: 2,000 Hz (+) and 500 Hz (−)
C: Acceleration level: 20 G_{rms} (+) and 10 G_{rms} (−)

The motion of the vibration shaker head was vertical; in this work we assume that this motion is on the *y* axis of a three-dimensional Cartesian coordinate system, hence, the axis of vibration is the *y* axis (see Fig. 4). According to industry guidelines, electronics equipment should be tested in each of the equipment's three orthogonal axes (three orientations). It has been decided that these three orientations (orientations 1, 2, and 3 in Fig. 4) would be related to the axis of the vibration in order to identify the effect of the orientation of the wires on the vibration system. Therefore, each test replicated three times—one for each of the equipment's orthogonal axes (see Fig. 4). The duration of each test was 3 h (one hour per axis). One sample was used for each test and the total amount of samples used in the experimental process was 24.

Electrical resistance measurements were performed before and after testing on the devices using a four-point resistance probe system. The probes were placed on each of the two Au pads of each pair and the resistance values were recorded to identify any changes in resistivity. Each recorded value represented the total resistance of all the wires of each pair.

Downloaded from http://meridian.allenpress.com/jmep/article-pdf/10/2/80/2240810/imaps_376.pdf by guest on 31 October 2022

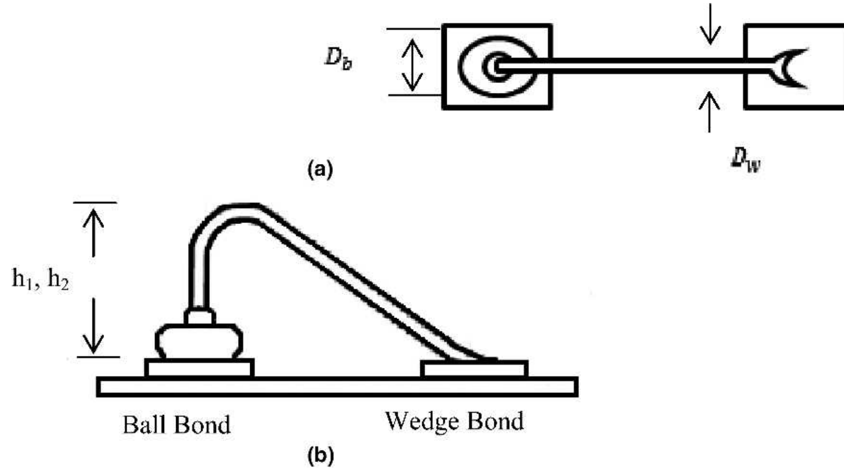

Fig. 2. Schematic representation of the wire bonding structure (a) top view and (b) side view.

Table I
Wire Bonding Parameters and Levels

	Description	Unit	Small loop	Large loop
First bond (ball bond)	Ultrasonic time	ms	80	81
	Ultrasonic power	W	1.55	1.55
	Force	g(f)	55	57
Second bond (wedge bond)	Ultrasonic time	ms	75	74
	Ultrasonic power	W	2	2
	Force	g(f)	100	89

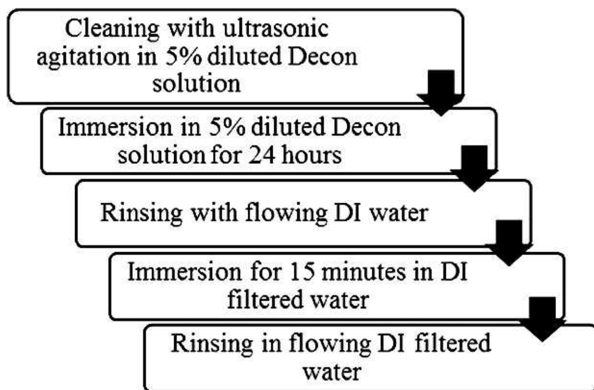

Fig. 3. Cleaning protocol for Au thick film substrates on alumina prior to wire bonding.

Mechanical testing was performed using the ASTM F 1269-06 [12] test method for destructive shear testing of the ball bonds. An untested substrate was used for the baseline shear force measurements. After testing, the wire bonds were subjected to shear testing in order to verify acceptance based on minimum values set by the ASTM F 1269-06 test method. Errors occurred during the shear testing process that mostly involved misalignment of the testing tool behind the bond, which led to invalid shear force levels. Consequently, the shear force values for some bonds have not been obtained. Only the valid values for the shear forces to failure are presented in this paper.

Visual inspection was performed using the MIL-STD 883 [13] for examining the geometry of bond contacts such as wire lift-offs and the adhesion and metallization, the loop geometry, and any potential wire deformation.

Results and Analysis

A. Electrical Characterization

Electrical resistance measurements revealed a considerable decrease in the resistance of the wires for the two different

Table II
Orthogonal Array and Control Factors Assignment
(Symbols − and + Represent the Low and High Levels of the Control Factors)

Test number	Process parameter level		
	A	B	C
1	−	−	−
2	+	−	−
3	−	+	−
4	+	+	−
5	−	−	+
6	+	−	+
7	−	+	+
8	+	+	+

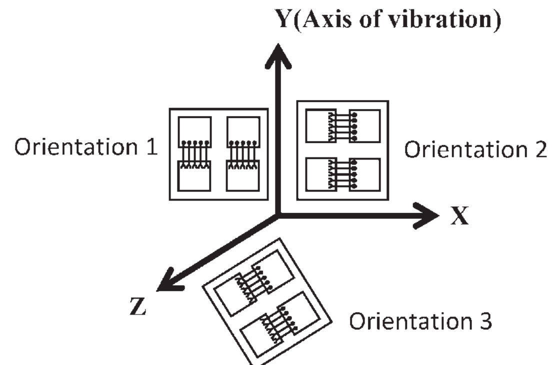

Fig. 4. Wire orientations with respect to the axis of vibration during testing.

Downloaded from http://meridian.allenpress.com/jmep/article-pdf/10/2/80/2240810/imaps_376.pdf by guest on 31 October 2022

loop heights after vibration/temperature testing. Clearly, that was an indication of some type of change occurring in the wires or bonds during testing.

The results for the resistance measurements for the small loop are shown in Fig. 5. From the 24 samples tested, only two showed an increase in electrical resistance. The first sample was the one tested at 120°C, 500 Hz, 10 G_{rms} on the *x* axis. The increase rate in that case was 7.1%. An increase in the resistance also occurred after testing at 250°C, 2,000 Hz, 20 G_{rms} on the *y* axis. Here the increase rate was only 0.41%. The resistance for the remaining 22 samples showed a decrease, ranging from 0.06% to 20.42%. The maximum decrease occurred when testing at 250°C, 500 Hz, 20 G_{rms} on the *x* axis and the minimum at 120°C, 500 Hz, 10 G_{rms} on the *y* axis. In general, samples tested at 500 Hz showed a considerably higher rate in the decrease of electrical resistance. Also, the average decrease of those samples was 7.83%.

Fig. 6 shows the results for the resistance measurements for the larger loop height. Here the resistance was reduced in all the samples. The maximum decrease occurred after testing at 250°C, 500 Hz, and 20 G_{rms} on the *x* axis, which is consistent with the results from the small loop measurements. The minimum decrease occurred at 250°C, 500 Hz, and 10 G_{rms} on the *y* axis, which is also the axis of vibration. The average decrease here was 9.70%.

B. Mechanical Testing

Shear testing was performed on an untested sample for each loop height. As shown in Fig. 7, only one bond in each case failed to exceed the industry's minimum shear gram force (hereafter referred to as g(f)) of 30 g(f) [12]. It is believed that

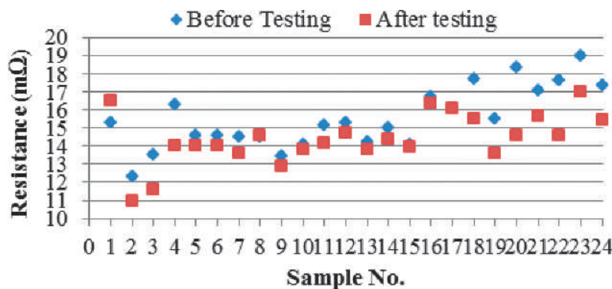

Fig. 5. Electrical resistance changes for the small loop wires (♦) before and (■) after testing.

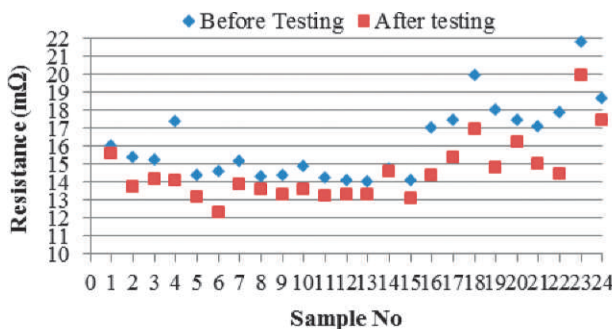

Fig. 6. Electrical resistance changes for the large loop wires (♦) before and (■) after testing.

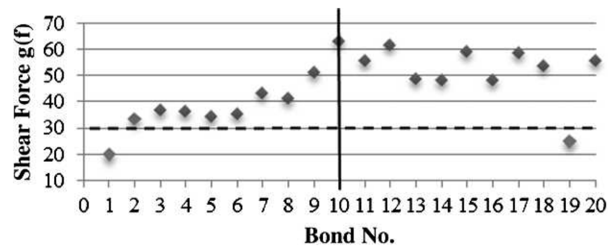

Fig. 7. Shear force values of bonds before testing.

this is probably due to a poor interface between the bond and the pad.

The diagrams in Fig. 8 show the shear force measurements of the bonds after testing at the eight different combinations of conditions. The effect of the different levels of temperature, frequency, and acceleration on the bond strength is clear.

The largest number of bonds that did not meet the 30 g(f) shear load was observed after testing at 250°C, 500 Hz, and 20 G_{rms} (see Fig. 8f). Here 13 out of 25 bonds failed to exceed the minimum level of bond shear load and the ones that were successful had shear loads relatively close to the limit. As shown in Table III, the average shear load in this case was 28.72 g(f), which was the lowest recorded shear load measurement, with a standard deviation of 6.13 g(f).

Another case was after testing at 250°C, 500 Hz, and 10 G_{rms} (see Fig. 8b). Even though only seven bonds failed here, all the other bonds had shear strengths at an average of 35 g(f) with a standard deviation of 7.96 g(f).

Similarly, bonds that tested at the lower frequency level were the ones that mostly failed or had shear forces relatively close to the industry minimum. Additionally, in the case where the temperature was at 250°C, the amount of bonds that had shear loads to failure of <30 g(f) was larger. Furthermore, the acceleration levels also had an effect on the bond strength; higher acceleration resulted in lower strength levels.

In the cases where the frequency level was at 2,000 Hz, bonds had high strength levels—most of them well above the industry's minimum—while the number of bonds that had shear loads to failure of <30 g(f) was small. In the two cases where the temperature was at 250°C—either at 10 G_{rms} or 20 G_{rms}—5 out of the 25 bonds failed instead of one or two when the temperature was at 120°C.

The wire loop height effects are not clear in the diagrams after testing. Note, however, that the force levels for the large loop wires were considerably lower than for the small loop wires after testing. As it will be seen in the section that follows, the most severe degradation of the bonds and the wires occurred at the large loop wires.

The wire orientation with respect to the axis of vibration also had an effect on the bond strength. Most failures, and the lowest strength values, were recorded on the samples where the wires were vertically oriented to the axis of vibration.

To assist in the practical interpretation of these experiments, and to support the observations on the effects of the different combinations of loading conditions on the shear forces to failure, interaction plots on the main effects of the three factors involved in the experiment (temperature, frequency, acceleration) were created. In these three-way interaction plots, each

Downloaded from http://meridian.allenpress.com/jmep/article-pdf/10/2/80/2240810/imaps_376.pdf by guest on 31 October 2022

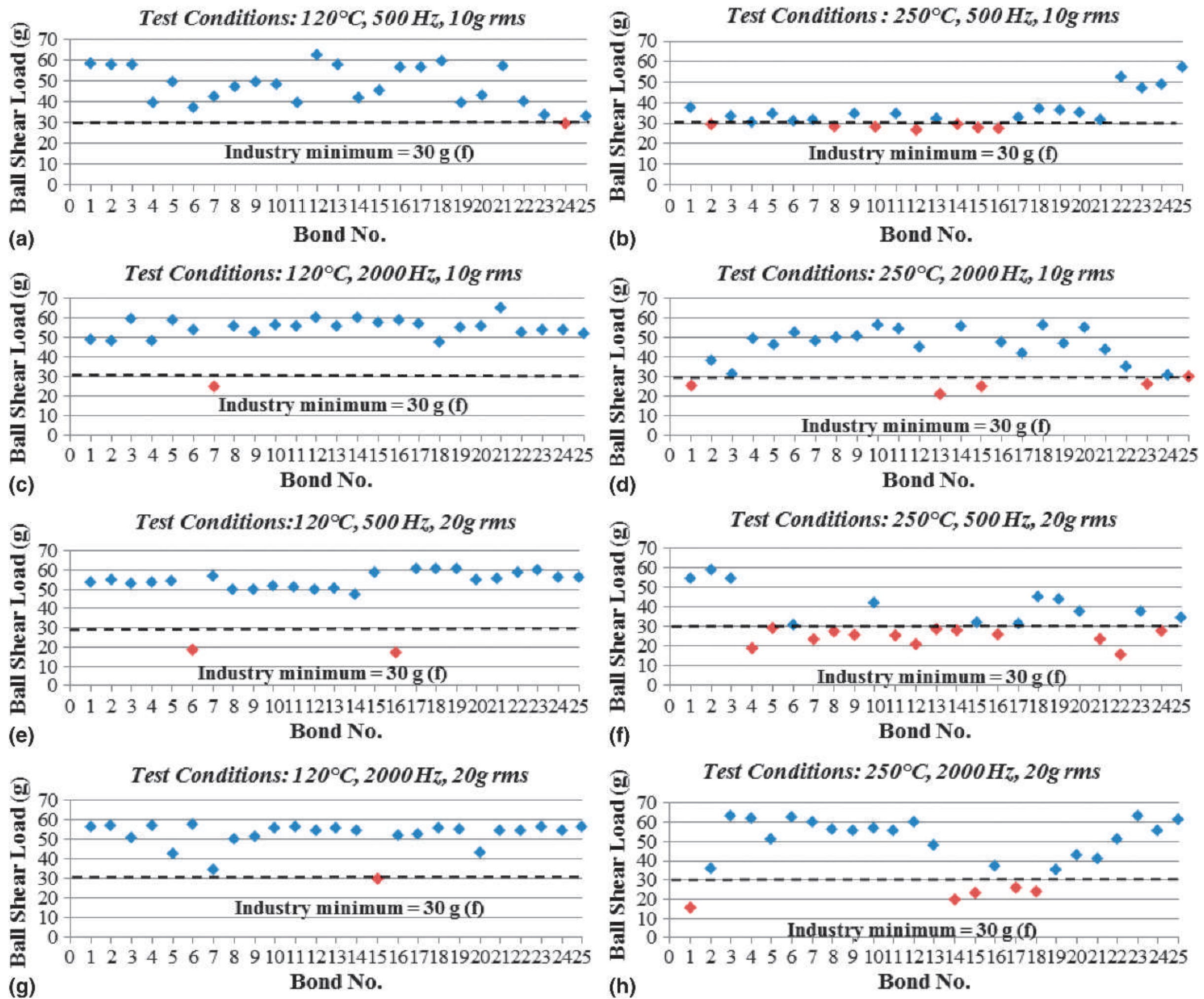

Fig. 8. Shear force values of bonds after testing at (a) 120°C, 500 Hz, 10 G_{rms}, (b) 250°C, 500 Hz, 10 G_{rms}, (c) 120°C, 2,000 Hz, 10 G_{rms}, (d) 250°C, 2,000 Hz, 10 G_{rms}, (e) 120°C, 500 Hz, 20 G_{rms}, (f) 250°C, 500 Hz, 20 G_{rms}, (g) 120°C, 2,000 Hz, 20 G_{rms}, (h) 250°C, 2,000 Hz, 20 G_{rms}.

Table III
Shear Load Mean Values and Standard Deviation for Bonds After Testing

Wire orientation on the vibration system	Ball bond shear failure load, g(f)	120°C 500 Hz 10 G_{rms}	250°C 500 Hz 10 G_{rms}	120°C 2,000 Hz 10 G_{rms}	250°C 2,000 Hz 10 G_{rms}	120°C 500 Hz 20 G_{rms}	250°C 500 Hz 20 G_{rms}	120°C 2,000 Hz 20 G_{rms}	250°C 2,000 Hz 20 G_{rms}
y	Mean	48.73	32.03	49.61	42.50	49.25	37.28	50.46	50.85
	SD	8.63	3.00	10.92	9.87	12.50	15.82	8.32	16.78
x	Mean	50.26	30.13	56.92	44.29	47.07	28.72	51.06	44.48
	SD	8.08	3.07	2.54	13.74	12.45	6.13	8.78	15.78
z	Mean	43.61	41.92	54.55	40.49	58.16	32.97	53.39	44.53
	SD	11.35	9.36	4.66	10.80	2.34	9.38	4.06	14.36
All bonds	Mean	47.38	34.98	53.73	42.35	51.76	32.99	51.70	46.54
	SD	9.62	7.96	7.30	11.17	10.84	11.20	7.06	15.25

plot represents the effect of two factors for each level of the third factor on the average shear force. Here we are interested in the lower average shear force values—the lower the shear force, the greater the effect of the loading conditions.

Fig. 9 provides a graphical representation of the average shear force as an effect of frequency and acceleration for the two temperature levels. Fig. 9a shows the main effects and interactions between the frequency and acceleration for the temperature level $T = 120°C$ and Fig. 9b for $T = 250°C$. There is a significant interaction between frequency and acceleration. The graph reveals that lower frequencies lead to lower shear force values. At higher temperatures (see Fig. 9b) the effect of

Downloaded from http://meridian.allenpress.com/jmep/article-pdf/10/2/80/2240810/imaps_376.pdf by guest on 31 October 2022

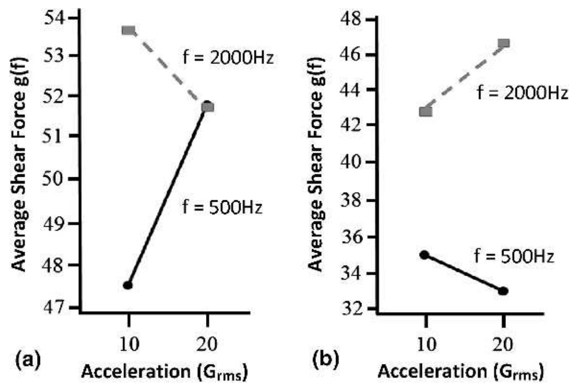

Fig. 9. Main effects and interaction plots for frequency and acceleration when (a) $T = 120°C$, and (b) $T = 250°C$.

lower frequencies in the shear force decrease is greater, especially at the higher acceleration level.

Fig. 10 shows the main effects and interaction plots between temperature and acceleration for the two levels of frequency. Even though the interaction between temperature and acceleration at higher frequencies is more significant (lines are not parallel), the effect in the decrease of the shear force is greater when the frequency is at its lower level—the average shear force is lower at this level.

Fig. 11 shows the main effects and interactions between the temperature and frequency for the two levels of acceleration. The parallel lines in Fig. 11a show no interaction between the

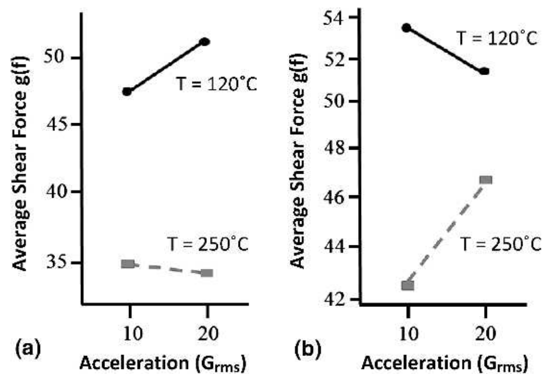

Fig. 10. Main effects and interaction plots for temperature and acceleration when (a) $f = 500$ Hz, and (b) $f = 2{,}000$ Hz.

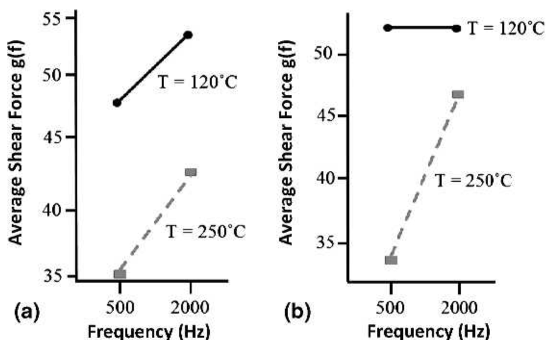

Fig. 11. Main effects and interaction plots for temperature and frequency when (a) $a = 10$ G_{rms}, and (b) $a = 20$ G_{rms}.

temperature and frequency at the low acceleration level while the nonparallel lines in Fig. 11b show a significant interaction at the high acceleration level. The observation that the combination of high temperature, low frequency, and high acceleration leads to the lowest shear force values can be supported in Fig. 11b by the great difference in the results of the shear force for the two frequency levels at the high temperature level.

C. Visual Inspection by Optical Microscopy

1) Observations from Failed Bonds After Shear Testing

Fig. 12 shows the failure mechanisms identified after observation of the bonds that were subjected to shear testing. The dominant failure mechanism in all the cases was ball shear between the ball bond and the Au thick film metallization. Fig. 12a is an example of this particular mechanism observed at a sample after testing at 250°C, 500 Hz, 10 G_{rms}.

After testing at either 250°C, 500 Hz, 10 G_{rms} or at 250°C, 500 Hz, 20 G_{rms}, ball shear with partial ball lift-off was observed. This mechanism was observed in both cases and Fig. 12b is a representative taken from a sample after testing at 250°C, 500 Hz, 10 G_{rms}.

Ball shear with partial metallization lift-off observed after testing at those conditions as well. Fig. 12c is an example of that mechanism after testing at 250°C, 500 Hz, 20 G_{rms} where most of the metallization lift-offs occurred.

2) Observations from Deformed Wires After Testing

Fig. 13a shows the wire deformation after testing at 120°C/250°C, 500 Hz, 10 G_{rms}/20 G_{rms} on the *x* axis. Note here that the *x* axis orientation is perpendicular to the direction of vibration. The wire deformation seems to follow a particular pattern; the wires are deformed only in one direction. This deformation was more severe in the large loop wires.

One of the wire deformation types that was observed after testing at 250°C, 500 Hz, 20 G_{rms}, *y* axis can be seen in Fig. 13b. Here one of the wires was sharply curved at the highest point of the wire loop (large loop).

Fig. 13c shows deformation of the wires on the *z* axis. It seems that here the wire deformation does not follow a particular direction; as can be seen in the figure, the wires are tangled sideways. This deformation observed in both cases where the conditions applied were 250°C, 500 Hz, 20 G_{rms} and 250°C, 500 Hz, 10 G_{rms}.

Another type of deformation observed after testing at 250°C, 500 Hz, 20 G_{rms}. The deformation of one of the wires was so severe that it touched the neighboring wire, causing a short circuit (see Fig. 13d).

Fig. 14 shows a wire lift-off. This failure observed on several samples after testing at 250°C, 500 Hz, 10 G_{rms}/20 G_{rms}, *x*/*y* axis; the one tested at 250°C, 500 Hz, 20 G_{rms} was the one where most of the wire lift-offs occurred in comparison with the others.

D. Combined Vibration/Temperature Tests on Wire Bonded SOI Devices

SOI test devices with op-amp functional blocks were assembled into high temperature cofired ceramic (HTCC) packages with 25 μm diameter Au wire. The gain of the op-amps was

Downloaded from http://meridian.allenpress.com/jmep/article-pdf/10/2/80/2240810/imaps_376.pdf by guest on 31 October 2022

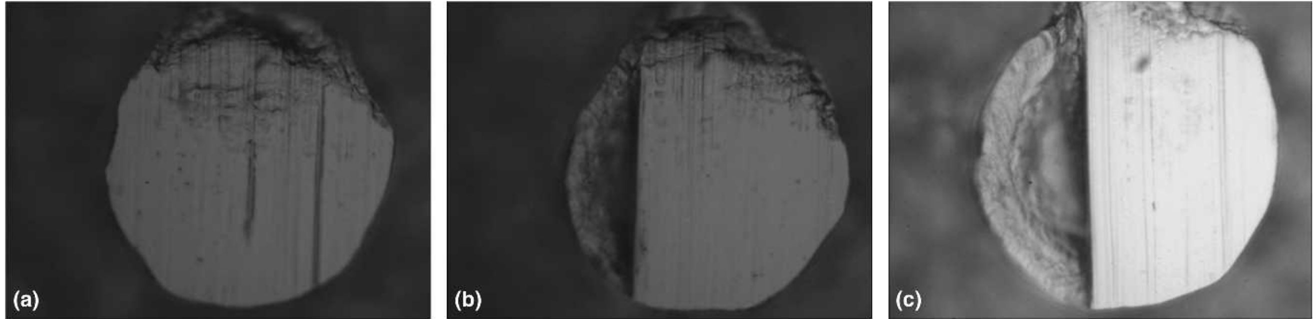

Fig. 12. Failure mechanisms identified from shear testing, (a) ball shear, (b) ball shear with partial bond lift-off, and (c) ball shear with partial metallization lift-off.

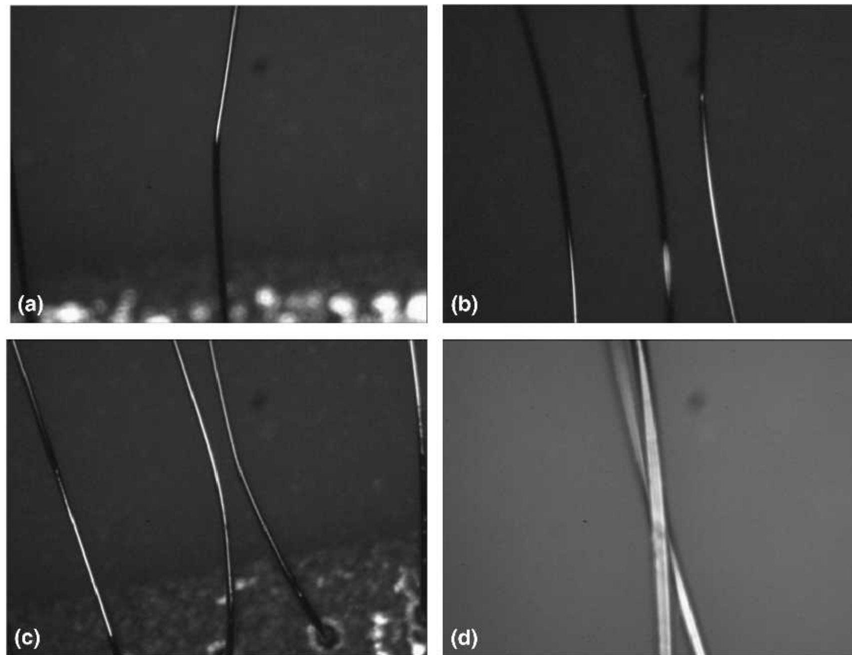

Fig. 13. Wire deformation on the (a) *x* axis, (b) *y* axis, (c) *z* axis, and (d) short circuiting caused by overlapping wires.

Downloaded from http://meridian.allenpress.com/jmep/article-pdf/10/2/80/2240810/imaps_376.pdf by guest on 31 October 2022

electrically measured prior to vibration testing at temperatures of 25°C, 125°C, and 250°C and electrically measured again after vibration testing at 25°C and 250°C at the same temperatures to assess the change in op-amp gain. The results showing the change in op-amp gain at test temperatures of 25°C, 125°C, and 250°C are presented in Table IV.

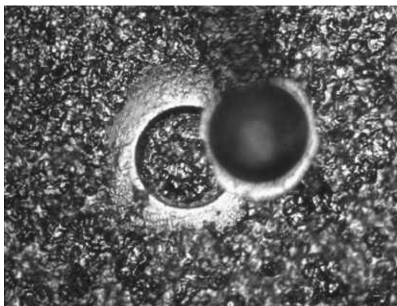

Fig. 14. Wire lift-off.

The results indicate that there was little discernible difference within ±5% in the op-amp gain between the vibration tests carried out at 25°C and 250°C.

Discussion

The system setup and testing methodology proved appropriate for ball bond evaluation under combined high temperature and vibration conditions. Electrical resistance changes gave an indication of some type of change occurring for the wires and wire bonds. Visual observation after testing revealed that the conditions applied had an effect on the wire bonding behavior and several failure modes were identified.

The resistance decrease in the wires after testing could be attributed to annealing of the wire at operating temperature rather than any specific failure mechanism caused by the vibration/temperature conditions. An initial decrease in resistance after short-term exposure was also observed by other researchers [14, 15].

Table IV
Change in Op-Amp Gain at Test Temperatures of 25°C, 125°C, and 250°C

Test conditions	Electrical test temperature °C	Op-amp 1	Op-amp 2	Op-amp 3
Vibration at 25°C	25	−1.05	−1.64	3.22
	125	0.33	0.60	0.87
	250	1.13	0.54	0.68
Vibration at 250°C	25	0.29	−5.13	1.57
	125	−1.40	−0.24	−2.83
	250	0.66	1.24	0.95

Note: Nominal gain on op-amps ×100.

In the combined vibration/temperature testing, the low frequency (high displacement) levels caused a general reduction in ball bond shear loads to failure. Furthermore, at a temperature of 250°C, the reduction in bond shear load to failure is bigger compared with 120°C. The vibration/temperature testing caused bond lift-off, a phenomenon that was expected from the reduction in shear load to failure that indicated that the ball bond/thick film metallization interface was affected, which resulted in a reduction in shear load to failure.

Deformation of the wires at the high displacement vibration conditions was also more severe.

Visual observation of the wires after testing proved the role that the wire orientation with respect to the vibration direction plays on the wire deformation. The deformation of the wires oriented vertically in relation to the axis of the vibration was more severe. Additionally, the number of wire lift-offs after testing in that case was bigger than in any other testing condition.

The current work has shown that the combined effect of vibration and temperature reduced the ball bond shear load to failure through a weakening effect at the ball bond/thick film interface. In more severe or extended vibration/temperature conditions, this may ultimately result in the occurrence of different types of failures in service. Further tests are planned to extend the combined vibration/temperature endurance tests and to assess the effect on wire bond pull strengths, where annealing of the wire above the ball bond may also result in changes in performance.

Note that the work presented in this paper was an attempt to cover the mechanical behavior of the wires and bonds; the focus was on the deformation of the wires and the strength of the bonds. It was a preliminary investigation in order to identify the basic needs for this type of testing and gain an initial understanding of the types of failures that occurred, so as to set the basis for future studies that cover all the aspects of the effects of the conditions applied. Thus, at this stage, the vibration response of the wires and bonds is not included in this work, but it was investigated by the authors, and the findings will be presented in the near future.

For wire bonds that were hermetically sealed in real devices, little difference was seen in the op-amp gain for the samples tested under vibration loading at 25°C and 250°C. It is likely that the devices need to have a prolonged exposure to combined vibration/temperature to accelerate potential end-of-life failure modes, where the wire bonds may become detached before any significant electrical effect is observed.

Summary and Conclusion

The work revealed some of the effects that the combined conditions of thermal and vibration loadings have on the wire bond integrity. The results have contributed to the understanding of the failure mechanisms that can occur on typical electronic circuits due to the combined effects of the aforementioned conditions. Particularly, it has been proven that low vibration frequencies and consequently high displacements cause severe deformation on the wires and the bonds. Failure at the interface between the wire bonds and the thick film metallization resulted in a reduction of the shear load to failure. Finally, the reduction in electrical resistance is attributed mostly to possible annealing of the wires due to high temperature.

A need has been identified to further investigate and focus on the aspects of minimizing the effects of combined temperature and vibration. Those aspects could include low loop heights and consequently shorter wires, minimizing and preferably avoiding resonance effects, and finally the environment surrounding the wire bonds. All these aspects are being investigated in the continuing study.

Acknowledgments

The authors thank Inseto Limited (Andover, UK) for their technical support and guidance through the wire bonding process and the Manufacturing Technology Centre (MTC; Ansty Park, Coventry, UK) for providing the facilities and assistance for the shear testing.

References

[1] G. Harman, *Wire Bonding in Microelectronics: Materials, Processes, Reliability, and Yield*, 2nd ed., McGraw Hill, New York, 1997.

[2] P. Matkowski and Q. Haiyu, "Vibration tests utilization in the study of reliability of connections in microelectronics," Proceedings of the International Students and Young Scientists Workshop, Photonics and Microsystems, pp. 61-64, 7-8 July 2005.

[3] D. Shepherd, P.S. Grant, C. Johnston, and S. Riches, "The behavior of Au-Au wire bonds in extreme environments," Paper presented at the International Conference on High Temperature Electronics (HiTEC), 2010.

[4] M.A. Bahi, H. Fremont, J.P. Landesman, A. Gentil, and P. Lecuyer, "A new methodology for the identification of ball bond degradation during high-temperature aging tests on devices in standard plastic packages," *Microelectronics and Reliability*, Vol. 49, pp. 1273-1277, 2009.

[5] P.A. Agyakwa, M.R. Corfield, L. Yang, J.F. Li, V.M.F. Marques, and C.M. Johnson, "Microstructural evolution of ultrasonically bonded high purity Al wire during extended range thermal cycling," *Microelectronics and Reliability*, Vol. 51, pp. 406-415, 2011.

[6] M. Mayer, J.T. Moon, and J. Persic, "Measuring stress next to Au ball bond during high temperature aging," *Microelectronics and Reliability*, Vol. 49, pp. 771-781, 2009.

[7] S. Murali, N. Srikanth, and C.J. Vath, "Effect of wire diameter on the thermosonic bond reliability," *Microelectronics and Reliability*, Vol. 46, pp. 467-475, 2006.

[8] F. Oldervoll and F. Strisland, "Wire bond failure mechanisms in plastic encapsulated microcircuits and ceramic hybrids at high temperatures," *Microelectronics and Reliability*, Vol. 44, pp. 1009-1015, 2004.

[9] H.A. Mustain, A.B. Lostetter, and W.D. Brown, "Evaluation of gold and aluminum wire bond performance for high temperature (500°C) silicon carbide (SiC) power modules," Proceedings of the 55th Electronic Components and Technology Conference (ECTC), Vol. 2, pp. 1623-1628, 2005.

[10] M. Mirgkizoudi, C. Liu, and S. Riches, "Reliability testing of electronic packages in harsh environments," Proceedings of the 12th Electronics Packaging Technology Conference (EPTC), pp. 224-230, 8-10 December 2010.

Downloaded from http://meridian.allenpress.com/jmep/article-pdf/10/2/80/2240810/imaps_376.pdf by guest on 31 October 2022

[11] K.A. Kamaludin, M. Mirgkizoudi, C. Liu, and S. Riches, "Effects of combined thermal and vibration loadings on wire bond integrity," Proceedings of the 12th International Conference on Electronic Packaging Technology & High Density Packaging (ICEPT-HDP), pp. 828-831, 2011.
[12] ASTM, "Standard test methods for destructive shear testing of ball bonds," *ASTM F 1269-06*, West Conshohocken, PA, 2007.
[13] USDOD, "Test method standard: Microcircuits," *Military Standard 883F, Method 2010.10*, Washington, DC, 2004.
[14] R. Johannessen, F. Oldervoll, and F. Strisland, "High temperature reliability of aluminium wire-bonds to thin film, thick film and low temperature co-fired ceramic (LTCC) substrate metallization," *Microelectronics and Reliability*, Vol. 48, pp. 1711-1719, 2008.
[15] M.A. Bahi, H. Fremont, J.P. Landesman, A. Gentil, and P. Lecuyer, "A new methodology for the identification of ball bond degradation during high-temperature aging tests on devices in standard plastic packages," *Microelectronics and Reliability*, Vol. 49, pp. 1273-1277, 2009.

Downloaded from http://meridian.allenpress.com/jmep/article-pdf/10/2/80/2240810/imaps_376.pdf by guest on 31 October 2022